ADVANCED FUNCTIONAL MATERIALS
www.afm-journal.de

Facile Fabrication of Two-Dimensionally Ordered Macroporous Silver Thin Films and Their Application in Molecular Sensing

By *Guosong Hong, Cheng Li,* and *Limin Qi**

Large-area, freestanding, two-dimensionally ordered macroporous (2DOM) Ag thin films with adjustable periodic spacings and good mechanical robustness were fabricated via nanosphere lithography at the solution surface (NSLSS) combined with interfacial reactions. The obtained 2DOM Ag thin films exhibited typical properties of plasmonic crystals with well-resolved reflectivity dips and vivid colors. The facile NSLSS method enabled the 2DOM Ag thin films to be readily transferred to arbitrary substrates to realize application as thin film sensors. Their application as both a surface plasmon resonance (SPR) sensor and a surface-enhanced Raman scattering (SERS) sensor in the detection of both small molecules and biological macromolecules were explored. As SERS substrates for the detection of 4-aminothiophenol (4-ATP) molecules, the 2DOM Ag thin films showed enhancement factors as high as the 10^7 order, which made them a promising sensor for the detection of trace amount of analyte adsorbed on the surface. As SPR sensors, the 2DOM Ag thin films modified with a self-assembled monolayer of recognizing molecules as binding sites showed remarkable shift in the reflectivity dips responsive to the chemical environments. When used for the specific detection of avidin molecules, the 2DOM Ag thin film biosensors exhibited excellent performance with low detection limit (≈100 pM) and broad working range (100 pM–200 nM), indicating that they may be a promising candidate for high-performance biosensors.

1. Introduction

Plasmonics is a flourishing new field of science and technology that focuses on light manipulation at the nanoscale through exploiting surface plasmons, which are coherent oscillations of conduction electrons excited by electromagnetic radiation near a metal-dielectric interface.[1–3] Owing to the evanescent electromagnetic field, the surface plasmons respond to the local refractive index with high sensitivity and thus offer opportunities for label-free molecular sensing and chemical imaging.[4] Ordered metal nanostructure arrays that are patterned periodically in two dimensions (2D) are usually referred to as plasmonic crystals, which provide a promising platform for sensing and imaging of surface binding events.[5] Untill now, a variety of methods have been developed for the fabrication of ordered arrays of metal nanostructures.[6] In particular, nanosphere lithography (NSL), which employs monolayer colloidal crystals (MCCs) as deposition or etch masks, represents an inexpensive and versatile bottom-up procedure for fabricating periodic nanostructure arrays on surfaces.[7,8] This NSL procedure was first developed by Van Duyne and co-workers to fabricate periodic arrays of metallic nanostructures with tunable structural parameters,[9] which was subsequently extended to the fabrication of periodic nanobowl/nanohole arrays of metals. For example, such metallic nanobowl/macropore arrays have been successfully fabricated by NSL methods employing MCC templates through electrodeposition,[10] solution dipping,[11] photochemical technique,[12] and thermal evaporation.[13] Nevertheless, it remains a challenge to develop facile NSL routes to plasmonic crystals with desirable structures and high performance in plasmonic applications.

Generally, surface plasmon resonance (SPR) sensing and surface-enhanced Raman scattering (SERS) are two typical sensing techniques based on plasmonic crystals. SPR spectroscopy is a well-known detection method to monitor the surface binding events in real time, which gives rise to the changes in the dielectric environment at the surface.[6] The traditional SPR method makes use of the properties of surface plasmons in the form of propagating surface plasmon polaritons (SPPs), which is difficult to be integrated into portable, low-cost devices and high-throughput systems. Notably, plasmonic crystals made of nanoparticle and nanohole arrays of plasmonic materials give rise to localized surface plasmon resonances (LSPRs), which can be tuned by carefully controlling the size, shape, and spacing of the nanostructures. In contrast to propagating SPPs, LSPRs are confined around the objects being excited and can have higher intensity and spatial resolution.[4] In this

[*] G. Hong, C. Li, Prof. L. Qi
Beijing National Laboratory for Molecular Sciences (BNLMS)
State Key Laboratory for Structural Chemistry
of Unstable and Stable Species
College of Chemistry
Peking University
Beijing 100871, P. R. China
E-mail: liminqi@pku.edu.cn

DOI: 10.1002/adfm.201001177

regard, Dahlin et al. detected the existence of NeutrAvidin with ultralow detection limit through functionalization of randomly arranged gold nanohole arrays with biotin.[14] Rogers and co-workers fabricated the quasi-3D plasmonic crystals composed of square arrays of gold cylindrical nanowells, which exhibited sensitive response to the adsorption of avidin on the surface of gold functionalized with biotin-LCBSA.[15] Recently, Vörös and co-workers reported the application of densely packed and optically coupled plasmonic particle arrays composed of gold spheroids in single-layer sensing of biomolecules, which adsorbed on gold surface via both non-specific physisorption and specific chemisorption.[16] While nanostructured metal films were fabricated via NSL and well-resolved plasmon resonances were observed in reflection spectra as reflectivity dips,[17] the application of such plasmonic crystals in SPR sensing has rarely been explored yet. It would be desirable to explore the feasible NSL approaches towards sensitive SPR sensors based on metallic nanobowl arrays or two-dimensionally ordered macroporous (2DOM) metal thin films.

Besides SPR sensing, SERS was also widely applied for analytical detection with high sensitivity and low detection limit. SERS provides us with a platform for the great enhancement in Raman scattering signals of the analyte molecules adsorbed on the SERS substrates, hence an SERS active substrate could not only be used as signal amplifier for the Raman spectra, but also be functionalized with ligand molecules for the SERS-based detection of trace amount of analyte that binds to the surface with specificity.[18] Roughened metal films have been widely used as SERS substrates with high enhancement factors but the application of SERS has been limited by poor reproducibility of the substrates. For obtaining SERS substrates with more reliable performance and reasonably large SERS enhancement factors, many efforts have been devoted to the fabrication of periodically arranged arrays of nanoholes in metallic thin film and metallic nanodots on substrate since these structures are more precisely defined and the periodic nanostructures are expected to enable an increase in transmission of light by several orders of magnitude.[19,20] As recent examples, Ag[21] and Au[22] nanocap arrays fabricated by sputtering the deposited materials onto the template were used to compare the SERS performances with different periodic spacings. Using the Ag thin films over nanospheres as SERS substrates, Van Duyne et al. developed the detection for glucose[23] and biomarker[24] from the SERS signal of both analytes on Ag surface. It may be noted that most of the 2D metallic nanoarrays used for SPR-based sensors or SERS substrates were fabricated by direct sputtering the metallic materials with lithographic templates. It is worthwhile to develop facile solution routes towards high-quality 2D metallic nanoarrays. Moreover, it would be desirable to realize the integration of SPR-based sensing and SERS-based sensing into one single sensor based on periodically structured metallic materials.

Herein, we report the fabrication of large-area, free-standing, 2DOM Ag thin films with adjustable periodic spacings and good mechanical robustness via nanosphere lithography at the solution surface (NSLSS), which is convenient, cost-effective and productive. Moreover, their application as both an SPR sensor and an SERS sensor in the detection of different chemical and biological molecules has been explored. It has been shown that the obtained 2DOM Ag thin films provide a promising candidate for molecular sensing with compatibility towards different kinds of analytes, low detection limit and broad working range.

2. Results and Discussion

2.1. Characterization of 2DOM Ag Thin Films

2DOM Ag thin films were fabricated via the NSLSS method based on colloidal lithography at the solution surface combined with interfacial reactions, which was originally developed for the fabrication of free-standing, through-pored nanonets of inorganic materials.[25] The protocol for the fabrication of 2DOM Ag thin films is schematically illustrated in **Scheme 1**. At first, hexagonal-close-packed (hcp) monolayer colloidal spheres self-assembled on silicon wafer were transferred to the surface of $AgNO_3$ aqueous solution to form floating MCC. Then, the gas-solution reaction between reducing gaseous molecules and aqueous silver ions took place under the spatial confinement of the MCC template. When Ag^+ ions in the solution were reduced to form Ag nanoparticles, the nucleation would preferentially occur heterogeneously at the gas-solution and solution/solid interfaces, hence the deposition of Ag occurred mostly at the lower surface of the spheres immersed in the $AgNO_3$ solution and at the triangular interstices among every three neighboring spheres. After an adequate reaction time (e.g., 24 h), the formed MCC-Ag composite was picked up and then immersed in an organic solvent to remove the MCC template, resulting in the formation of free-standing 2DOM Ag thin film showing good mechanical robustness, which enabled us to handle it with tweezers (Figure S1, Supporting Information). Due to the asymmetrical deposition of Ag on the MCC template, the obtained Ag thin films normally possessed two sides, i.e., the obverse side exposed to the vapor phase where Ag rarely

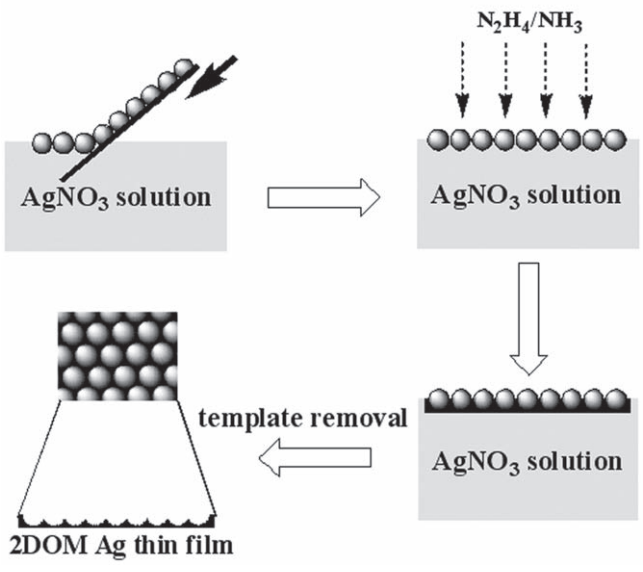

Scheme 1. Protocol for the preparation of 2DOM Ag thin film via the NSLSS method.

deposited, and the reverse side immersed in the solution where Ag deposited most. It can be seen that the obverse side exhibited vivid reflection colors due to plasmon resonances whereas the reverse side exhibited only the characteristic metallic luster of Ag (Figure S1, Supporting Information).

Figure 1 shows typical scanning electron microscopy (SEM) images, X-ray diffraction (XRD) pattern, and reflection spectrum of the 2DOM Ag thin films obtained by using an MCC template made of 450 nm spheres. The vertical top views of the obverse side show highly ordered hexagonally arranged circular macropores with a long-range periodicity, and obvious triangular top surface that duplicates the interspace among colloidal spheres (Figure 1a,b). It is also shown that the resulting 2DOM thin film exhibits a periodic spacing (i.e., the distance between the centers of two neighboring pores) of 450 nm, identical to the diameter of the colloidal spheres, indicating that the Ag deposition at the tangent point between two neighboring spheres had little effect on the close packing of the spheres. Tilted top views of the Ag thin film further verify the ordered macroporous structures and clearly show the triangular top surface (Figure 1c,d). This ordered Ag nanopillar array with triangular platelet on each top of the pillars is well aligned preserving the hexagonal pattern of the MCC template. The side view shown in Figure 1e suggests that the porous thin film has an apparent thickness of about 0.5 μm. Figure 1f shows a bottom view of the Ag thin film, which suggests that the thin film has a continuous, rough reverse face while it has a highly porous obverse face, in good agreement with the observed two different colors. Figure 1g shows the XRD pattern of the obtained 2DOM thin film, which exhibits sharp reflections characteristic of metallic Ag with the cubic structure, demonstrating the formation of 2DOM thin film composed of pure silver. It is known that the plasmon resonances of plasmonic crystals can be observed in reflection spectra as dips because the energy of surface plasmon polariton waves is dissipated as ohmic loss in the metals.[5] The representative reflection spectrum of the obtained 2DOM Ag thin film is shown in Figure 1h, which exhibits a sharp dip at 440 nm and a broad dip around 750 nm due to the plasmonic resonances, indicating its characteristic of plasmonic crystals.

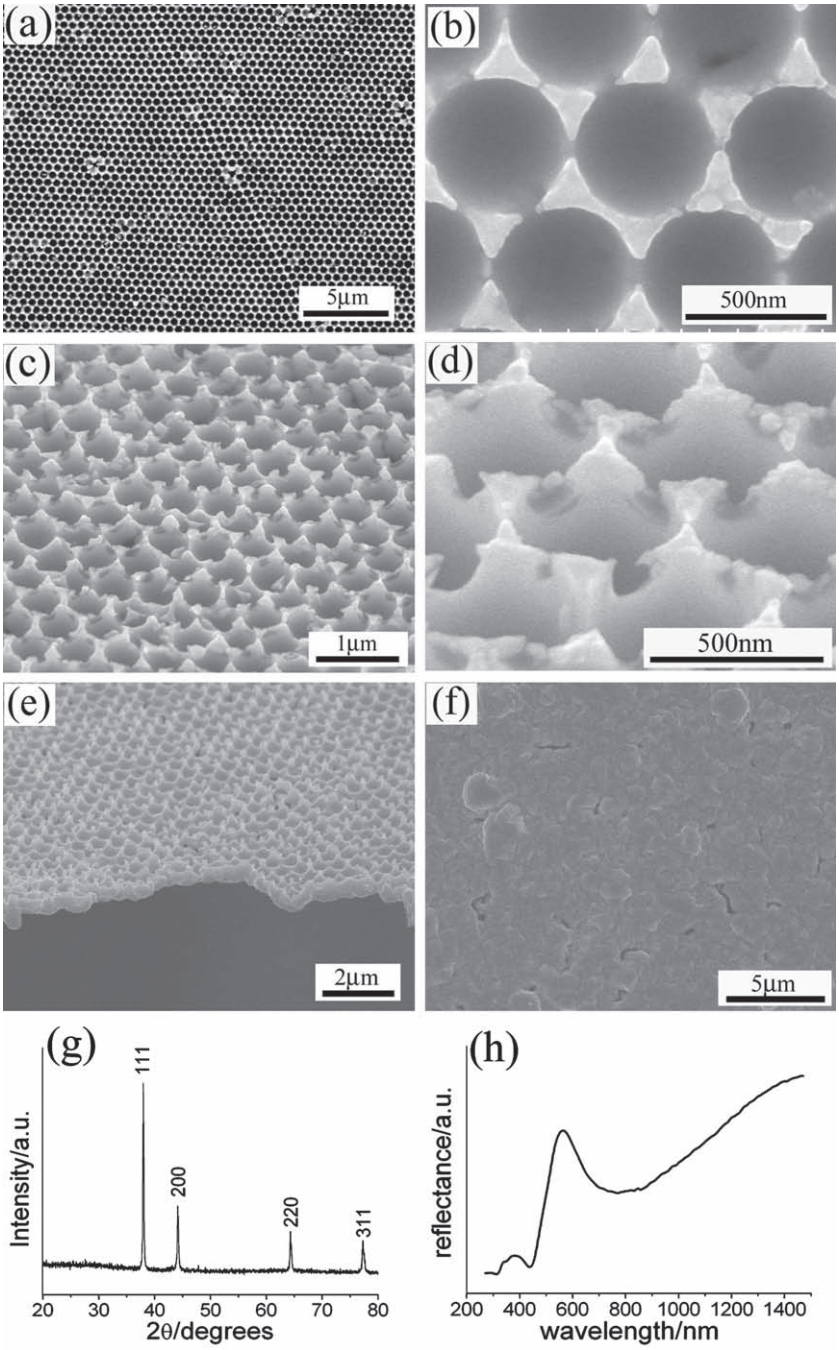

Figure 1. SEM images (a–f), XRD pattern (g), and reflection spectrum (h) of 2DOM Ag thin films with a periodic spacing of 450 nm. SEM images were observed from different directions: a,b) vertical top view; c,d) tilted top view; e) side view; f) bottom view.

In order to reveal the formation mechanism of the 2DOM Ag thin film, the original MCC template and the MCC-Ag composite film were also characterized by SEM observation (**Figure 2**). SEM image shown in Figure 2a presents a single crystalline domain of hexagonally assembled 450 nm colloidal spheres in the MCC template, which was then transferred to the solution surface to spatially confine the Ag deposition. Top views of the resultant MCC-Ag composite film clearly show that triangle-shaped deposits filled the interstices among every three PS spheres (Figure 2b,c). The side view shown in Figure 2d suggests that besides the controlled deposition of Ag at the cross section with solution surface, significant deposition of

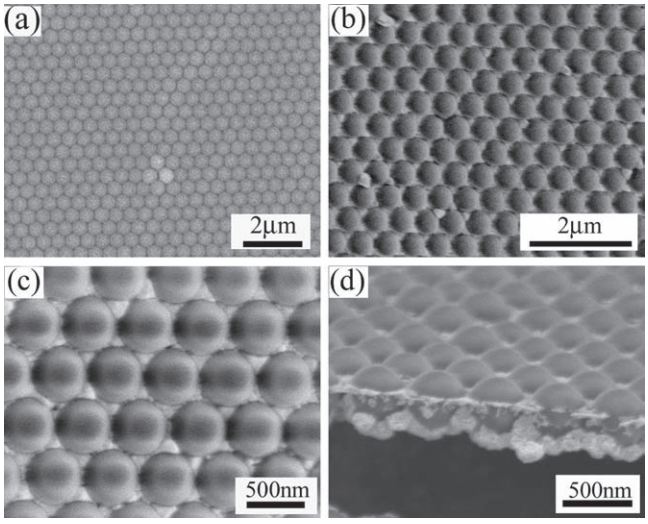

Figure 2. SEM images of 450 nm MCC template (a) and the templated MCC-Ag composite by top view (b,c) and side view (d).

Ag on the lower hemispheres occurred, leading to the continuous Ag film with rough surface, which is consistent with the overall morphology of the final 2DOM Ag thin film after template removal (Figure 1). The formation of this asymmetric film could be attributed to the excessive deposition of Ag nanoparticles during the reaction since the reverse side of the film was immersed in the reactant solution all the time. It may be noted that the continuous Ag nanoparticles on the reverse side, although randomly arranged, enabled the film with high mechanical strength, which made it possible to transfer the Ag thin film to any substrate without structural destruction and to handle it easily with tweezers. Moreover, the configuration of the reverse side may not impose any negative effect on its application as molecular sensor since the output signals arising from SPR or SERS will only be acquired from the light reflectance or scattering from the obverse side.

It was found that the composition of the diffusive reducing vapor had a pronounced effect on the morphology of the Ag thin film fabricated by the NSLSS method. For the fabrication of the above-described, well-defined 2DOM Ag thin film, a mixture of strong aqua ammonia and concentrated hydrazine solution with a volume ratio of 3:7 was used as the source for gaseous reductant. If no NH_3 molecules were introduced into the diffusive gas, coarse 2DOM Ag thin film composed of large primary particles was obtained (Figure S2a,b, Supporting Information). Under this condition, through-pored Ag nanonets could be produced at a shorter reaction time and a suitable diffusion rate of the N_2H_4 gas.[25] If a small amount of NH_3 was introduced to the diffusive gas (i.e., the volume ratio between strong aqua ammonia and concentrated hydrazine solution was kept at 1:9), the size of the primary Ag particles constituting the 2DOM thin film was considerably decreased and the surface of the Ag film looked more smooth (Figure S2c,d, Supporting Information). These results indicate that NH_3 molecules played an important role in the fabrication of 2DOM Ag thin films with delicate nanostructures although N_2H_4 alone acted as reductant in the reaction at solution surface. We propose that in the presence of an appropriate amount of diffusing NH_3 gas, the $Ag(NH_3)_2^+$ complex ions rather than the hydrated Ag^+ ions reacted with reductive N_2H_4 vapor to form the Ag deposits. Since $Ag(NH_3)_2^+$ complex ions were less vulnerable to reductants compared to hydrated Ag^+ ions, the nucleation and growth of Ag would be slower, resulting in the smoother Ag replica consisting of smaller nanoparticles. However, if the NH_3 proportion in diffusive reductive gas was too high, no continuous Ag film could be obtained possibly because of the partial dissolution of the deposited Ag nanoparticles by excess NH_3.

The NSLSS method exhibited versatility in the fabrication of 2DOM Ag thin films with periodic spacings ranging from submicrometer to micrometer region. By varying the colloidal sphere diameter of the MCC template, the periodic spacing and the pore diameter of the 2DOM Ag thin films could be readily adjusted. For example, 2DOM Ag thin films with spacings of 130 nm, 600 nm, 800 nm, and 1000 nm were fabricated by using the MCC templates made of colloidal spheres with the diameters identical to the spacings (Figure S3, Supporting Information). All the reflectance spectra of these 2DOM Ag thin films show reflectivity dips corresponding to their different SPRs. While the Ag thin films with spacings less than 600 nm exhibit two well-resolved dips in the wavelength range 400–1400 nm, multiple dips are evident for those with spacing larger than 800 nm. Generally, with increasing the periodic spacing, the number of the reflectance minimums (i.e., the dips) increases. Similar reflectance spectra were obtained for the nanostructured metal films fabricated by NSL combined with electrochemical deposition.[17] It has been shown that plasmon resonances of plasmonic crystals can be tuned by exploiting intrinsic factors such as material type, unit cell size, and lattice symmetry as well as extrinsic factors such as the incident light excitation directions and local dielectric environments.[5] Basically, all the sharp dips can be used for molecular sensing since their position are sensitive to the molecules adsorbed on the Ag surface.

2.2. SERS-Based 2DOM Ag Thin Film Sensors

Taking into account the excellent SERS performance of metal Ag as well as the 2DOM structures that may provide "hot spots" to further enhance the Raman signals, it was reasonably expected that the obtained 2DOM Ag thin films could act as effective SERS substrates for the detection of trace amount of molecules adsorbed on the surface. In this regard, we measured the SERS signals of 4-aminothiophenol (4-ATP) molecules chemically adsorbed on the obverse surface of the 2DOM Ag thin films with different periodic spacings, which are presented in **Figure 3**. It can be seen that compared with the normal Raman spectrum of solid 4-ATP, noticeable changes in the frequency shift and relative intensity of the bands could be observed from the SERS spectra of the 2DOM Ag thin films. The shifted Raman scattering peaks located at 1006 cm^{-1}, 1078 cm^{-1}, 1187 cm^{-1}, 1473 cm^{-1}, and 1577 cm^{-1} corresponded to the a_1 vibration mode, while the other peaks at 1141 cm^{-1}, 1307 cm^{-1}, 1389 cm^{-1} and 1438 cm^{-1} corresponded to the b_2 vibration mode.[26,27] All the 2DOM Ag thin films showed excellent enhancing performance in the SERS spectra, especially for the b_2 vibration mode, which could be ascribed to the charge transfer from the metal

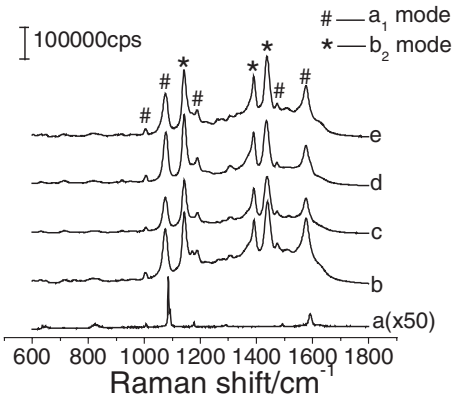

Figure 3. a) Raman spectrum of solid 4-ATP. b–e) SERS spectra of 4-ATP molecules adsorbed on the obverse side of 2DOM Ag thin films with different periodic spacings: b) 130 nm; c) 450 nm; d) 600 nm; e) 1000 nm.

to the adsorbed molecules.[27] The enhancement factors (EFs) of the 2DOM Ag thin films with different spacings can be calculated using the following equation:

$$\mathrm{EF} = \frac{N_{\mathrm{bulk}}\, I_{\mathrm{surf}}}{N_{\mathrm{surf}}\, I_{\mathrm{bulk}}}$$

where N_{bulk} and N_{surf} represent the number of 4-ATP molecules in the bulk solid sample and on the surface of the 2DOM Ag thin films, respectively; and I_{bulk} and I_{surf} denote the Raman scattering intensities from the solid 4-ATP and the 4-ATP SAMs adsorbed on the surface. Based on the measured values, the EFs (**Table 1**) for different substrates at two typical Raman shift peaks that represent the a_1 vibration mode and b_2 vibration mode, respectively, were calculated and listed in Table 1 (For calculation details, see SI). It can be clearly seen that no matter how large the periodic spacing was, all the 2DOM Ag thin films exhibited excellent performance in the Raman scattering enhancement of 4-ATP molecules, which could be potentially applied in the detection of trace amount of target analytes.

Interestingly, the SERS performances of our substrates appeared to be dependent on the periodic spacing or the feature size. In particular, when the periodic spacing is decreased from 1000 nm to 450 nm, the EF values in both a_1 and b_2 modes gradually decrease. However, a remarkable increase in EF can be observed when the spacing is further decreased to 130 nm and the Ag thin film with a spacing of 130 nm even exhibited the most prominent enhancement in a_1 mode. The size-dependent SERS properties have also been observed for the Au nanohole and nanodisk arrays with different feature sizes, which were ascribed to varying degrees of electromagnetic coupling between the holes.[28] Similarly, the electromagnetic field in the current 2DOM Ag thin film could also be modulated via the coupling effect induced from variation in feature sizes. When the spacing is decreased from 1000 nm to 450 nm, electromagnetic coupling would be weakened, leading a gradual decrease in EF. If the spacing is further decreased to 130 nm, the triangular area, which would act as the hot spots in SERS, becomes quite small in size, and hence remarkably enhances the electromagnetic field nearby,[29] resulting in a considerable increase in EF.

It can be seen from Table 1 that EF values around 10^7 order in the b_2 mode can be obtained for the obtained 2DOM Ag thin films with different periodic spacings. Compared with the reported EF values for 4-ATP molecules adsorbed on various Ag nanostructures used as SERS substrates, the EF values obtained from the current 2DOM Ag thin films are extremely high. For example, Wang et al. reported the SERS performance of Ag nanoplates arranged on different substrates, with their EF values lower than 10^6 for 4-ATP molecules;[30] Li et al. prepared Ag film through DNA-network-templated self-assembly of silver nanoparticles and then measured the EF value for 4-ATP molecules enhanced on the Ag film as 10^5;[31] the EF value for 4-ATP molecules adsorbed on the Ag nanoparticles deposited on porous anodic alumina was measured to be 5×10^5.[32] Besides the 4-ATP molecule, other molecules such as 4-mercaptobenzoic acid, 3,4-dichlorobenzenethiol, 1,4-benzenedithiol, and benzenethiol were also used as SERS probes on the surface of various Ag structures. For example, Van Duyne et al. have carried out study on the SPR extinction maxima dependent SERS substrates composed of Ag nanoparticles arrays derived from NSL, which demonstrated that the largest EF values for derivative benzenethiols could reach as high as 10^7 order.[33] The EF value for 4-mercaptobenzoic acid molecules on the surface of Ag film electrochemically deposited in ionic liquid could reach 1.0×10^6,[34] whereas hexagonally ordered array of Ag nanocaps prepared from silica MCC template gave an EF value of 1.8×10^7 towards the adsorbed benzenethiol molecules.[35] Therefore, the EF values measured for the 4-ATP molecules adsorbed on the 2DOM Ag thin films are comparable to the highest EF values reported for various SERS probes on Ag structures. Such high EF values could be attributed to the coupling of SPR between the neighboring macropores and the periodic "hot spots", which may be favorable for the detection of certain analytes at ultra low concentration.

Table 1. EF values of 2DOM Ag thin films with different periodic spacings for a_1 and b_2 vibration modes at 1577 cm^{-1} and 1438 cm^{-1}.

Periodic spacing (nm)	EF values	
	a_1 mode at 1577 cm^{-1}	b_2 mode at 1438 cm^{-1}
130	2.0×10^6	1.1×10^7
450	1.1×10^6	0.9×10^7
600	1.3×10^6	1.0×10^7
1000	1.6×10^6	1.2×10^7

2.3. SPR-Based 2DOM Ag Thin Film Sensors

The position of the dips in the reflectance spectra of the 2DOM Ag thin films is very sensitive to the molecules adsorbed on their surface, which endows them with promising applications in molecular detection. In order to improve the molecular selectivity and sensitivity, we first introduced a self-assembled monolayer of recognizing molecules onto the surface of the 2DOM Ag thin films as binding sites for the targeted analytes. In this regard, thiol groups are usually required for the

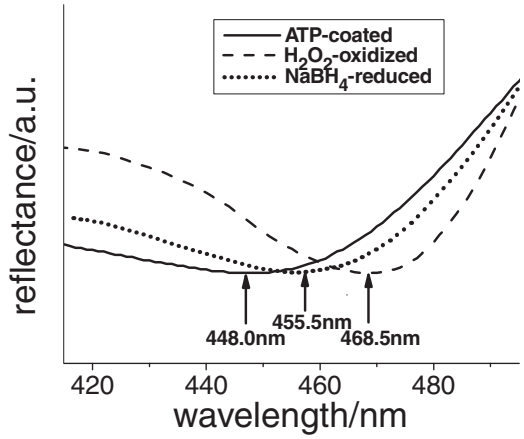

Figure 4. Reflectance spectra of 2DOM Ag thin films activated by modification with 4-ATP, oxidized by H_2O_2, and reduced by $NaBH_4$.

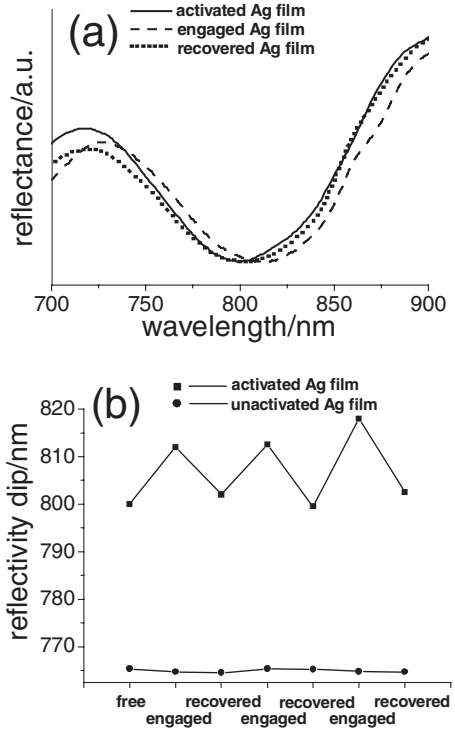

Figure 5. a) Reflectance spectra of 2DOM Ag thin films activated by modification with 3-MPA, engaged by adsorption of decylamine, and recovered by washing with acetic acid. b) Relationship between the reflectivity dip position and the status of the activated Ag thin films together with the variation of dip position with the status of the unactivated Ag thin films that were not treated with 3-MPA.

recognizing molecules to bind to the Ag surface via chemical interaction. As an example, the surface of the Ag thin film can be modified with the SAM of 4-ATP molecules that carry thiol groups, which were vulnerable to the oxidizing environments and could be easily oxidized to the product with a higher polarity, thereby increasing the surface RI and inducing a red shift in the reflectivity dips. Therefore, the 2DOM Ag thin films modified with 4-ATP may be used as a sensor to detect oxidants in the environment. As shown in **Figure 4**, after modification with 4-ATP, the 2DOM Ag thin film with a spacing of 450 nm exhibited a sharp dip at 448 nm, which had a red shift compared with the reflectivity dip for the unmodified 2DOM Ag thin film (440 nm). After soaking the 4-ATP modified Ag thin film in 1M aqueous H_2O_2 solution for barely 5 min, this dip red-shifted to 468.5 nm with a shift value as high as 18.5 nm. This oxidation-responsive sensor could be partially recovered to the reduced form after soaking in $NaBH_4$ solution, which could reduce some of the surface molecules back to the original 4-ATP molecules, resulting in a blue shift of the reflectivity dip to 455.5 nm. In this case, the 2DOM Ag thin film-based sensor exhibited its ability to sensitively respond to the oxidizing and reducing environments. As a control, if the original 2DOM Ag thin film without 4-ATP modification was immersed in 1 M H_2O_2 solution, only neglectable shift of the reflectivity dip can be observed. This control experiment demonstrated that a monolayer of adsorbed 4-ATP molecules was indispensable to the sensitive responsibility towards the oxidizing and reducing environments.

Similarly, the 2DOM Ag thin film modified with suitable recognizing molecules could be used as a sensitive sensor to detect amine molecules in the solution. In this case, the sharp dip at 765 nm for the 2DOM Ag thin film with a spacing of 1000 nm was selected as the indicator and 3-mercaptopropionic acid (3-MPA) was used as the recognizing molecule that can bind to the Ag surface through the thiol groups and bind to amine molecules through the carboxylic groups. As shown in **Figure 5**a, after activated by modification with 3-MPA molecules, the 2DOM Ag thin film exhibited a dip at 800 nm, which drastically red-shifted from 765 nm. Then, decylamine molecules were selected as analytes since their long alkyl chains could probably cause considerable shift in the reflectivity dip due to the relatively large change in the dielectric environment near the metal surface. After the activated 2DOM Ag thin film was exposed to decylamine in ethanol for 5 min and then rinsed with pure ethanol, the dip further red-shifted to a longer wavelength as a response of amine molecules that bound to the carboxylic groups in 3-MPA molecules via acid-base interaction. Recoverability for this amine sensor was tested by rinsing the Ag thin film engaged with decylamine in acetic acid. Figure 5a shows that the 2DOM Ag thin film recovered from the engaged status since the reflectivity dip blue-shifted back to the initial position before analyte binding. Interestingly, the amine sensor showed good repeatability up to three cycles, switching between the engaged status and the recovered status (Figure 5b), which enabled us to use the same Ag thin film several times for the amine detection. The control experiment shown in Figure 5b demonstrated that if the 2DOM Ag thin film was not activated by modification with 3-MPA beforehand, the Ag thin film would not have the capacity for amine detection. Obviously, the surface modification of 2DOM Ag thin film with 3-MPA molecules endowed the film with the ability and selectivity for amine detection. However, since the reaction between the carboxylic groups and amines is not specific towards the amine molecules with different alkyl chains, it remains a problem to discriminate different amines by this method.

Aside from the small molecules that could be detected through the dip shift due to chemical interactions at the surface of 2DOM Ag thin films, large biomolecules could also give rise to considerable shift in the reflectivity dip when binding to the SAMs on the surface of 2DOM Ag thin films via biological affinity. This affinity involves the biospecific interactions between the binding sites at the surface and the targeted analytes introduced externally, which could endow the 2DOM Ag thin film biosensors with high selectivity and low detection limit. The preparation procedure and operating principle for the 2DOM Ag thin film biosensor used for the detection of avidin via the specific binding between biotin and avidin is schematically shown in **Scheme 2**. First of all, we selected the biotin-avidin pair as model molecules to study the biosensing efficiency of the Ag thin film since the biotin-avidin system is a powerful tool with a high degree of affinity and specificity. In the preparation procedure for the Ag thin film-based biosensor, the functionalization of the Ag surface with biotinylated bovine serum albumin (biotin-LC-BSA) was a crucial step to activate the thin film, that is, to render the biosensor high specificity to avidin analyte. Therefore, it is very important to immobilize the biotin group onto the Ag surface via covalent binding between the free mercapto group in BSA and the silver atoms on the film surface. After removal of physically adsorbed biotin-LC-BSA with water, the Ag thin film could be considered as chemically modified with an SAM of biotin-LC-BSA molecules (namely, activated) and could be used to detect avidin molecules in solution. After the Ag thin film was immersed in avidin solution, the biotin groups on the Ag surface captured the avidin molecules to form biotin-avidin bindings to immobilize them on the Ag surface. Removal of free avidin molecules with weak physical adsorption was also required to detect the net adsorption of avidin molecules.

Taking the 2DOM Ag thin film with a spacing of 450 nm as an example, here we investigated the application of this Ag thin film as biosensor for the detection of avidin based on the specific binding between biotin and avidin. **Figure 6**a shows the reflectance spectra of the thin film biosensors at different states. It suggests that after modification with biotin-LC-BSA, the original reflectivity dip of the unmodified Ag film at 440 nm slightly red-shifted to 442 nm, resulting from the replacement of air with biotin-LC-BSA SAMs. It was noted that the incubation in biotin-LC-BSA solution for longer time would not induce any further shift in the dip for the modified 2DOM Ag thin film biosensor, indicating that the weak physisorption of biomacromolecules would not bring about detectable dip shift due to the absence of strong specific binding. Then the Ag thin film biosensor was incubated in 2 mL of aqueous avidin solution with different concentrations for 20 min. The reflection spectra of the thin film biosensor capturing avidin were measured after removal of free avidin molecules. A red shift of the reflectivity dip from 442 nm to 448 nm was clearly observed when 200 nM avidin solution was employed. It may be noted that the dip shift induced by avidin adsorption was relatively lower compared with those induced by 4-ATP oxidation and decylamine adsorption as shown in Figure 4 and 5, respectively. The exact reason remains unclear but a possible explanation could be that compared with the adsorption of a layer of macromolecules, the chemical change in a self-assembled monolayer of small molecules could induce larger change in the 2D periodic variation of dielectric environment for the 2DOM Ag thin film. However, such a shift in reflectivity dip is already large enough to enable quantitative sensing of avidin molecules.

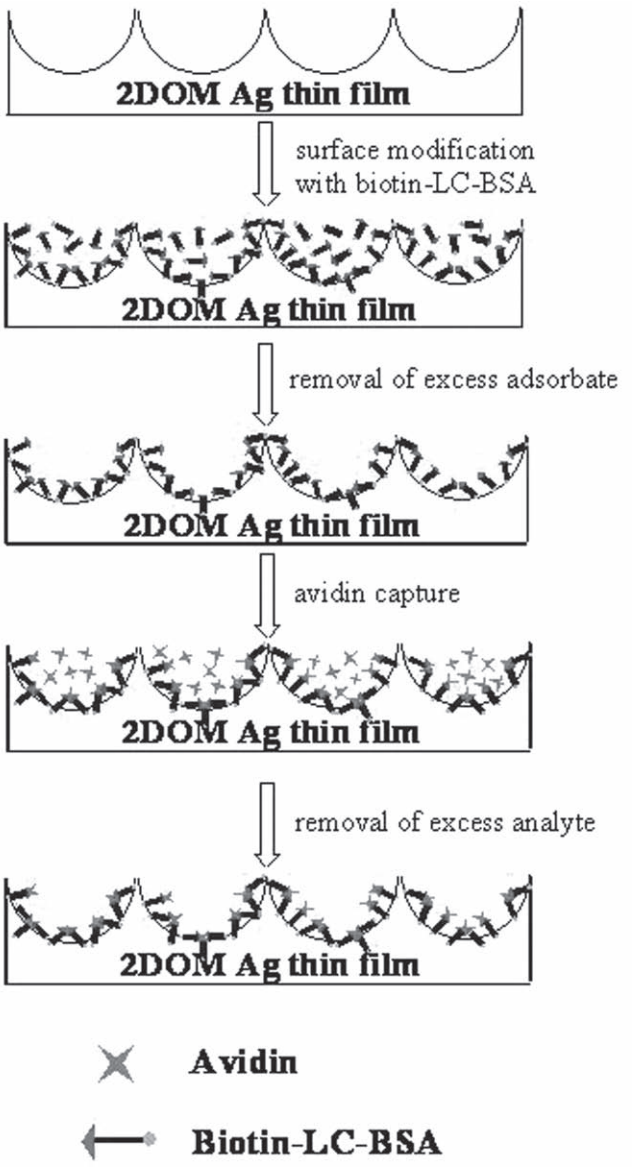

Scheme 2. Procedure for the preparation and operation of biosensor based on 2DOM Ag film for the detection of avidin molecules. The blue cross star with four dents represents the avidin molecule, which can bind to four molecules carrying biotin moiety (shown as red triangle) with affinity and specificity; the biotin-LC-BSA molecule consists of three parts as simplified in this cartoon, with the red triangle representing the biotin group, orange dot representing mercapto group in BSA that binds to Ag surface, and black bar symbolizing protein residue in BSA.

In order to reveal the capability of the Ag thin film biosensor for quantitative detection of avidin molecules, we investigated the relationship between dip shift due to the specific adsorption of avidin molecules on the activated 2DOM Ag thin films and the avidin concentration in solution. Figure 6b exhibits the

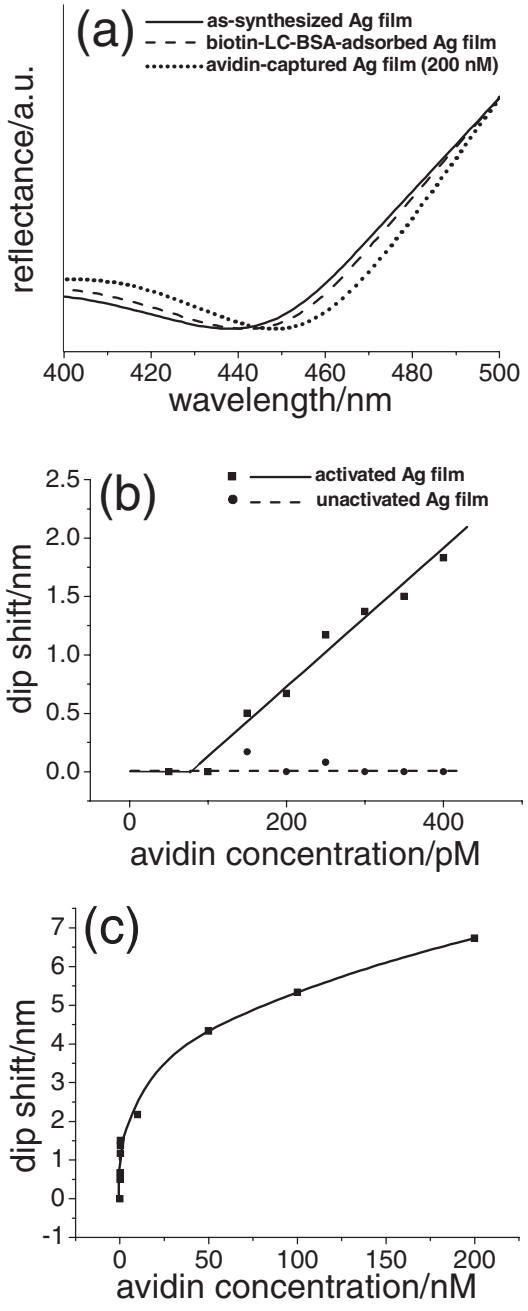

Figure 6. a) Reflectance spectra of 2DOM Ag thin film biosensors with different adsorbed molecules. b,c) Relationship between the reflectivity dip position and the avidin concentration in the concentration range of 0–400 pm (b) and the range of 0–200 nm (c). For comparison purpose, the situation of the unactivated Ag film without activation with biotin-LC-BSA is also shown in (b).

concentration dependence of the red shifts in spectral minimum measured from reflectance spectra at avidin concentrations lower than 400 pM. It can be seen that when the avidin concentration was below 100 pM, no detectable dip shift was observed in the reflectance spectra. The signal output in dip shift increased almost linearly with increasing avidin concentration when the avidin concentration was larger than 100 pM, indicating a detection limit as low as ≈100 pM. The linear fit for this low concentration area indicated that the detection sensitivity was about 5.8×10^{-3} nm/pM. To experimentally certify that the detection of avidin was exclusively based on the specific affinity of avidin molecules to the surface with binding sites composed of capture ligands, control experiments using the unactivated 2DOM Ag thin film without surface modification were carried out at different avidin concentrations. As shown in Figure 6b, if the surface of the Ag thin film was not activated with an SAM of ligand molecules, such as biotin-LC-BSA, the nonspecific interaction between the naked Ag surface and avidin molecules would not capture the avidin molecules chemically, thereby giving no detectable red shift in reflectivity dip. Therefore, the specific biotin–avidin interaction was crucial for the detection of avidin with high specificity.

However, at relatively high avidin concentrations, the curve considerably deviated from linearity (Figure 6c), which could be rationalized by considering that the adsorption of avidin molecules would become more and more difficult due to limited space with increasing avidin concentration. It should be pointed out that even though the relationship at high concentrations did not maintain the linearity, the variation curve was still reliable and could be used for quantitative determination of the avidin concentration. Therefore, from the detection limit around 100 pM to 200 nM, which was near the saturation point, the fabricated 2DOM Ag thin film biosensor showed a broad working range through at least three orders of magnitude. When compared with the detection limits and working ranges reported for the detection of avidin in the literature, the present Ag thin film biosensor exhibited high performance in both parameters. Most of the work reported for the detection of avidin based on noble metal nanostructures concerned the measurement of SPR absorption of these plasmonic materials. For example, based on the SPR absorption, Ag nanoparticle arrays fabricated via nanosphere lithography by Van Duyne et al. could reach the detection limit of 1 pM for streptavidin, but the working range for this detector was limited to a ≈1 pM–100 pM region.[36] Similarly, when colloidal Au modified onto optical fibres was used to detect streptavidin, the detection limit could reach 100 pM,[37] which was comparable to the result we obtained in Ag thin film biosensors, but this optical fibre sensor saturated in its response at 30 nM. Avidin-induced aggregation of biotin-modified Au colloids was also widely employed for sensing since the SPR absorption would be affected by the aggregation. For instance, Geddes et al. applied microwave for the ultrafast detection of streptavidin with the detection limit at about 5 nM.[38] Angular-dependent SPR was also applied to detect the analyte-induced aggregation with the detection limit of 5 nM for streptavidin.[39] In addition to the SPR-based biosensors, scientists have also utilized the stop bands of three-dimensionally ordered macroporous (3DOM) photonic crystals for the detection of certain biological molecules via surface specific adsorption; however, the as-reported sensors generally showed narrow working range in only one order of magnitude from the detection limit to the saturated signal.[40,41] Besides the ultralow detection limit for avidin analyte and the broad working range, another advantage for the 2DOM Ag film biosensor may be the short response time (≈20 min) when compared to the 3DOM photonic crystal sensors (≈2 h),[41] mainly because the 2D open

macropores offered easier accessibility for the analyte molecules to attach onto the surface.

3. Conclusions

Large-area, freestanding, 2DOM Ag thin films with adjustable periodic spacings and good mechanical robustness have been successfully fabricated via colloidal lithography at the solution surface combined with interfacial reactions, which is convenient, cost-effective and productive. The obtained 2DOM Ag thin films exhibited typical properties of plasmonic crystals with well-resolved reflectivity dips and vivid reflection colors. Their application as both an SPR sensor and an SERS sensor in the detection of both small molecules and biological macromolecules has been explored. As an SERS substrate for the detection of 4-ATP molecules, the 2DOM Ag thin films showed enhancement factors as high as the 10^7 order, which made them a promising sensor for the detection of trace amount of analyte adsorbed on the surface. As SPR-based sensors, the 2DOM Ag thin films showed remarkable shift in the spectral minimum responsive to the chemical environments. When used for the detection of small molecules, sensitive and repeatable signal output and easy recovery was achieved for the Ag thin film sensors. When used for the specific detection of avidin molecules, the Ag thin film biosensors exhibited excellent performance with low detection limit and broad working range. Since the surface of these 2DOM Ag thin films could be functionalized with SAMs of any desirable molecules, it can be envisioned that the sensors based on the 2DOM Ag thin films may find a wide range of applications in the detection of a tiny amount of analytes if suitable ligand-receptor couples can be introduced to the Ag surface. For example, screening of different viruses may be realized if the surface of the 2DOM Ag thin films can be modified with certain ligands to react differently with the receptors on the surface of the viruses.

4. Experimental Section

Assembly of the MCC Template at the Solution Surface: The MCC film was fabricated on a silicon wafer with easy transferability using a method recently developed at our lab.[42] In brief, a 20 μL water/ethanol dispersion containing monodisperse polystyrene (PS) or poly (styrene-methacrylic acid) (PS-PMAA) colloidal spheres was dropped onto the top surface of a 1 cm × 1 cm piece of glass surrounded by deionized water located at the mid-bottom of a Petri dish. Then the dispersion spread freely onto the water surface until it covered nearly the whole surface area, resulting in a colorful MCC film up to ≈25 cm^2 in area. A few microliters of SDS solution (2 wt%) was then dropped onto the water surface to lower the surface tension, which packed the MCC film on water surface closely. The MCC film was picked up with a 1 cm × 1 cm piece of silicon wafer and dehydrated naturally in the atmosphere. MCC templates with different sphere diameters and chemical compositions could be prepared in this way.

Synthesis of 2DOM Ag Thin Films: In a typical synthesis of 2DOM Ag thin films, the MCC film on 1 cm × 1 cm silicon wafer was first transferred onto the surface of 10 mM $AgNO_3$ aqueous reactant solution by inserting the loaded silicon wafer into the solution with an inclining angle. Then the vessel containing $AgNO_3$ aqueous solution with a piece of MCC film floating on the solution surface was placed in a closed desiccator where one vial containing 3 mL of strong aqua ammonia and 7 mL of hydrazine aqueous solution (85 wt%) acted as the source for gaseous reductant. The reaction was carried at room temperature for 24 h when the formed Ag film was continuous and robust to external force. Then the MCC-Ag composite film was picked up from the solution surface with an arbitrary substrate, rinsed with deionized water for 5 min, and dissolved in toluene or tetrahydrofuran (THF) twice with 10 min for each. Then the 2DOM Ag thin film with 1 cm × 1 cm square shape could be placed on any substrate or even handled with the tweezers.

Characterization: The samples were characterized by SEM (Hitachi FE-S4800, 2 kV), Hand XRD (RigakuD/MAX-PC2500, CuKα). All the reflectance spectra were measured by Hitachi U-4100 spectrophotometer with a 5 degree specular reflectance accessory, which enabled us to acquire the reflectance spectra of the obverse side of the 2DOM Ag thin films within a small circular window area of ≈2 mm diameter at an incident angle of 5°. All the film samples used for the optical measurement were derived from the original 1 cm × 1 cm Ag thin film directly obtained from the reaction vessel, by dividing the original piece into nine small pieces of ≈3 mm × 3 mm squares.

SERS Performance of 2DOM Ag Thin Films: For the preparation of SERS samples, the 4-ATP molecules were assembled onto the surface of 2DOM Ag thin films with different periodic spacings by immersing the Ag thin films into 2 mM ethanol solution of 4-ATP for 24 h to ensure the saturated coverage. Then the films were picked up from the solution and rinsed thoroughly with ethanol three times so as to remove the physically adsorbed 4-ATP molecules from the SAMs on Ag surface. Finally the Raman spectra of 4-ATP molecules on the 2DOM Ag thin films were measured with a Renishaw System 1000 Raman imaging microscope (Renishaw plc, U. K.) equipped with a 25 mW (632.8 nm) He-Ne laser (model 127–25RP, Spectra-Physics, USA) and a Peltier-cooled CCD detector (576 pixels × 384 pixels). A 50 × objective (NA = 0.80) mounted on an Olympus BH-2 microscope was used to focus the laser onto a spot of ≈1 μm diameter and the back-scattered light from the sample was collected.

Oxidation-Reduction Responsive Sensor Based on 2DOM Ag Thin Films: For the preparation of oxidation-reduction responsive Ag thin film sensor, the as-synthesized 2DOM Ag thin films of ≈3 mm × 3 mm squares were first immersed in 2 mM ethanol solution of 4-ATP for 24 h, and then rinsed three times in ethanol to remove the excess 4-ATP molecules. Reflectance spectra were then measured to ensure the 3-MPA molecules had been linked to the Ag surface. Afterwards, the thin film functionalized with 4-ATP was immersed in 1 M H_2O_2 aqueous solution for 5 min for oxidation, which could be detected as red shifts of spectral minimum in reflectance spectra. The oxidized thin film could be reduced via soaking in 1 M $NaBH_4$ aqueous solution for 10 min, which gave the signal as blue shift of reflectivity dip. Control experiments were carried using the as-synthesized 2DOM Ag thin films of ≈3 mm × 3 mm squares without surface functionalization with 4-ATP.

Decylamine Sensor Based on 2DOM Ag Thin Films: For the preparation of amine responsive Ag thin film sensor, the as-synthesized 2DOM Ag thin films of ≈3 mm × 3 mm squares were first immersed in 10 mM ethanol solution of 3-MPA for 24 h, and then rinsed three times in ethanol to remove the excess 3-MPA molecules. Reflectance spectra were then measured to ensure the 3-MPA molecules had been linked to the Ag surface. Afterwards, the thin film functionalized with 3-MPA was immersed in 1 M ethanol solution of decylamine for 5 min, rinsed with ethanol three times and measured for its reflectance spectra to give red shift in the reflectivity dip. The recovery of the film could be achieved by immersing the engaged film in acetic acid for at least 1 h, or treating the engaged film with hydrochloric acid for 5 min, which was followed by immersing the film in ethanol solution of 3-MPA again for 24 h. The reflectance spectra for recovered Ag film detector were also measured to give blue shift in the dip. Control experiments were carried using the as-synthesized 2DOM Ag thin films of ≈3 mm × 3 mm squares without surface functionalization with 3-MPA.

Avidin Biosensor Based on 2DOM Ag Thin Films: For the preparation of avidin responsive Ag thin film biosensor, the as-synthesized 2DOM Ag thin films of ≈3 mm × 3 mm squares were first immersed in 2 mg mL^{-1} biotin-LC-BSA solution for at least 16 h, and then rinsed with Milli-Q water for 5 min. Reflectance spectra were then measured to ensure the

biotin-LC-BSA molecules had been linked to the Ag surface. Afterwards, the thin film functionalized with biotin-LC-BSA was immersed in 2 mL aqueous avidin solution with different concentrations from 50 pM to 200 nM for 20 min, rinsed with Milli-Q water for 5 min. Then, its reflectance spectra were measured to give red shift in the reflectivity dip. Control experiments were carried using the as-synthesized 2DOM Ag thin films of ≈3 mm × 3 mm squares without surface functionalization with biotin-LC-BSA.

Supporting Information

Supporting Information is available from the Wiley Online Library or from the author.

Acknowledgements

This work is supported by NSFC (Grants 20873002, 20633010, and 50821061), MOST (Grant 2007CB936201), and SRFDP (Grant 20070001018). This article is part of a Special Issue on Nanomaterials Research by Chinese Scientists.

Received: June 10, 2010
Published online: October 5, 2010

[1] a) J. A. Schuller, E. S. Barnard, W. Cai, Y. C. Jun, J. S. White, M. L. Brongersma, *Nat. Mater* **2010**, *9*, 193; b) H. A. Atwater, A. Polman, *Nat. Mater* **2010**, *9*, 205.
[2] J. N. Anker, W. P. Hall, O. Lyandres, N. C. Shah, J. Zhao, R. P. Van Duyne, *Nat. Mater* **2008**, *7*, 442.
[3] H. Raether, *Surface Plasmons on Smooth and Rough Surfaces and on Gratings*, Springer-Verlag, Heidelberg, Germany **1988**.
[4] J. Yao, A.-P. Le, S. K. Gray, J. S. Moore, J. A. Rogers, R. G. Nuzzo, *Adv. Mater.* **2010**, *22*, 1102.
[5] H. Gao, W. Zhou, T. W. Odom, *Adv. Funct. Mater.* **2010**, *20*, 529.
[6] M. E. Stewart, C. R. Anderton, L. B. Thompson, J. Maria, S. K. Gray, J. A. Rogers, R. G. Nuzzo, *Chem. Rev.* **2008**, *108*, 494.
[7] Y. Li, W. Cai, G. Duan, *Chem. Mater.* **2008**, *20*, 615.
[8] G. Zhang, D. Wang, *Chem. Asian J.* **2009**, *4*, 236.
[9] a) T. R. Jensen, M. D. Malinsky, C. L. Haynes, R. P. Van Duyne, *J. Phys. Chem. B* **2000**, *104*, 10549; b) C. L. Haynes, R. P. Van Duyne, *J. Phys. Chem. B* **2001**, *105*, 5599.
[10] a) F. Q. Sun, W. P. Cai, Y. Li, B. Q. Cao, F. Lu, G. T. Duan, L. D. Zhang, *Adv. Mater.* **2004**, *16*, 1116; b) P. N. Bartlett, J. J. Baumberg, P. R. Birkin, M. A. Ghanem, M. C. Netti, *Chem. Mater.* **2002**, *14*, 2199.
[11] Y. Li, C. Li, S. O. Cho, G. Duan, W. Cai, *Langmuir* **2007**, *23*, 9802.
[12] F. Sun, J. Yu, *Angew. Chem. Int. Ed* **2007**, *46*, 773.
[13] M. Xu, N. Lu, H. Xu, D. Qi, Y. Wang, L. Chi, *Langmuir* **2009**, *25*, 11216.
[14] A. B. Dahlin, J. O. Tegenfeldt, F. Höök, *Anal. Chem.* **2006**, *78*, 4416.
[15] M. E. Stewart, N. H. Mack, V. Malyarchuk, J. A. N. T. Soares, T. -W. Lee, S. K. Gray, R. G. Nuzzo, J. A. Rogers, *Proc. Natl. Acad. Sci.* **2006**, *103*, 17143.
[16] T. Sannomiya, P. K. Sahoo, D. I. Mahcicek, H. H. Solak, C. Hafner, D. Grieshaber, J. Vörös, *Small* **2009**, *5*, 1889.
[17] P. N. Bartlett, J. J. Baumberg, S. Coyleb, M. E. Abdelsalam, *Faraday Discuss* **2004**, *125*, 117.
[18] J. P. Camden, J. A. Dieringer, J. Zhao, R. P. Van Duyne, *Acc. Chem. Res.* **2008**, *41*, 1653.
[19] T. W. Ebbesen, H. J. Lezec, H. F. Ghaemi, T. Thio, P. A. Wolff, *Nature* **1998**, *391*, 667.
[20] A. G. Brolo, E. Arctander, R. Gordon, B. Leathem, K. L. Kavanagh, *Nano Lett.* **2004**, *4*, 2015.
[21] T. Qiu, W. Zhang, X. Lang, Y. Zhou, T. Cui, P. K. Chu, *Small* **2009**, *5*, 2333.
[22] X. Liu, C.-H. Sun, N. C. Linn, B. Jiang, P. Jiang, *J. Phys. Chem. C* **2009**, *113*, 14804.
[23] K. E. Shafer-Peltier, C. L. Haynes, M. R. Glucksberg, R. P. Van Duyne, *J. Am. Chem. Soc.* **2003**, *125*, 588.
[24] X. Zhang, M. A. Young, O. Lyandres, R. P. Van Duyne, *J. Am Chem. Soc.* **2005**, *127*, 4484.
[25] C. Li, G. Hong, L. Qi, *Chem. Mater* **2010**, *22*, 476.
[26] Y. Wang, H. Chen, S. Dong, E. Wang, *J. Chem. Phys.* **2006**, *125*, 044710.
[27] Q. Zhou, G. Zhao, Y. Chao, Y. Li, Y. Wu, J. Zheng, *J. Phys. Chem. C* **2007**, *111*, 1951.
[28] Q. Yu, P. Guan, D. Qin, G. Golden, P. M. Wallace, *Nano Lett.* **2008**, *8*, 1923.
[29] M. Moskovits, *J. Chem. Phys.* **1978**, *69*, 4159.
[30] Y. Wang, X. Zou, W. Ren, W. Wang, E. Wang, *J. Phys. Chem. C* **2007**, *111*, 3259.
[31] G. Wei, L. Wang, Z. Liu, Y. Song, L. Sun, T. Yang, Z. Li, *J. Phys. Chem. B* **2005**, *109*, 23941.
[32] Z. Lu, W. Ruan, J. Yang, W. Xu, C. Zhao, B. Zhao, *J. Raman Spectrosc.* **2009**, *40*, 112.
[33] C. L. Haynes, R. P. Van Duyne, *J. Phys. Chem. B* **2003**, *107*, 7426.
[34] P. He, H. Liu, Z. Li, Y. Liu, X. Xu, J. Li, *Langmuir* **2004**, *20*, 10260.
[35] S. G. Jang, D.-G. Choi, C.-J. Heo, S. Y. Lee, S.-M. Yang, *Adv. Mater.* **2008**, *20*, 4862.
[36] A. J. Haes, R. P. Van Duyne, *J. Am. Chem. Soc.* **2002**, *124*, 10596.
[37] S.-F. Cheng, L.-K. Chau, *Anal. Chem.* **2003**, *75*, 16.
[38] K. Aslan, C. D. Geddes, *Anal. Chem.* **2007**, *79*, 2131.
[39] K. Aslan, P. Holley, L. Davies, J. R. Lakowicz, C. D. Geddes, *J. Am. Chem. Soc.* **2005**, *127*, 12115.
[40] W. Qian, Z.-Z. Gu, A. Fujishima, O. Sato, *Langmuir* **2002**, *18*, 4526.
[41] Y. Zhao, X. Zhao, J. Hu, M. Xu, W. Zhao, L. Sun, C. Zhu, H. Xu, Z. Gu, *Adv Mater.* **2009**, *21*, 569.
[42] C. Li, G. Hong, P. Wang, D. Yu, L. Qi, *Chem. Mater.* **2009**, *21*, 891.